

VAN3 ARF–GAP-mediated vesicle transport is involved in leaf vascular network formation

Koji Koizumi^{1,*†}, Satoshi Naramoto^{2,†}, Shinichiro Sawa^{2,†}, Natsuko Yahara³, Takashi Ueda², Akihiko Nakano^{2,3}, Munetaka Sugiyama⁴ and Hiroo Fukuda^{2,5,‡}

¹Department of Bioscience, Faculty of Applied Bioscience, Tokyo University of Agriculture, 1-1-1 Sakuragaoka, Setagaya-ku, Tokyo 156-8502, Japan

²Department of Biological Sciences, Graduate School of Science, The University of Tokyo, 7-3-1 Hongo, Bunkyo-ku, Tokyo 113-0033, Japan

³Molecular Membrane Biology Laboratory, RIKEN, 2-1 Hirosawa, Wako-shi, Saitama 351-0198, Japan

⁴Botanical Gardens, Graduate School of Science, The University of Tokyo, 3-7-1 Hakusan, Bunkyo-ku, Tokyo 112-0001, Japan

⁵Plant Science Center, RIKEN, 1-7-22 Suehiro-cho, Tsurumi-ku, Yokohama-shi, Kanagawa 230-0045, Japan

*Present address: Department of Botany, University of Toronto, 25 Willcocks Street, Toronto ON, M5S 3B2, Canada

†These authors contributed equally to this work

‡Author for correspondence (e-mail: fukuda@biol.s.u-tokyo.ac.jp)

Accepted 27 January 2005

Development 132, 1699–1711

Published by The Company of Biologists 2005

doi:10.1242/dev.01716

Summary

Within the leaf of an angiosperm, the vascular system is constructed in a complex network pattern called venation. The formation of this vein pattern has been widely studied as a paradigm of tissue pattern formation in plants. To elucidate the molecular mechanism controlling the vein patterning process, we previously isolated *Arabidopsis* mutants *van1* to *van7*, which show a discontinuous vein pattern. Here we report the phenotypic analysis of the *van3* mutant in relation to auxin signaling and polar transport, and the molecular characterization of the VAN3 gene and protein. Double mutant analyses with *pin1*, *emb30-7/gn* and *mp*, and physiological analyses using the auxin-inducible marker DR5::GUS and an auxin transport inhibitor indicated that VAN3 may be involved in auxin signal transduction, but not in polar auxin transport. Positional cloning identified VAN3 as a gene that encodes an adenosine diphosphate (ADP)-ribosylation factor-guanosine triphosphatase (GTPase) activating protein (ARF–GAP). It resembles animal ACAPs and contains four

domains: a BAR (BIN/amphiphysin/RVS) domain, a pleckstrin homology (PH) domain, an ARF–GAP domain and an ankyrin (ANK)-repeat domain. Recombinant VAN3 protein showed GTPase-activating activity and a specific affinity for phosphatidylinositols. This protein can self-associate through the N-terminal BAR domain in the yeast two-hybrid system. Subcellular localization analysis by double staining for Venus-tagged VAN3 and several green-fluorescent-protein-tagged intracellular markers indicated that VAN3 is located in a subpopulation of the trans-Golgi network (TGN). Our results indicate that the expression of this gene is induced by auxin and positively regulated by VAN3 itself, and that a specific ACAP type of ARF–GAP functions in vein pattern formation by regulating auxin signaling via a TGN-mediated vesicle transport system.

Key words: *Arabidopsis*, Mutant, VAN3, Vein, Vascular tissue, ARF–GAP

Introduction

The plant vascular system, which is composed of specialized conducting tissues, the xylem and phloem, forms a continuous network throughout the plant body and provides transport pathways for water and various solutes, including signaling molecules. In dicotyledonous plants, venation is reticulate, consisting of a midvein, secondary veins branching from the midvein and minor (tertiary and quaternary) veins that interconnect veins of higher orders or form open ends. Although venation appears to be richly diverse among different plant groups, this might be attributable to many small variations in vein branching and interconnections. A common basic mechanism is believed to underlie the spatial arrangement of vascular differentiation that generates venation.

Auxin has been nominated as a key molecule in the basic

mechanism controlling venation. A large number of studies indicate that polar auxin transport plays a crucial role in continuous vascular pattern formation (Nelson and Dengler, 1997; Berleth et al., 2000; Sachs, 2000; Aloni, 2001; Dengler, 2001; Tuner and Sieburth, 2002; Ye, 2002). The administration of chemicals that specifically inhibit polar auxin transport resulted in the formation of local aggregates of vascular cells in the marginal regions of newly developing leaves (Mattson et al., 1999; Sieburth, 1999). However, such inhibitors were less effective in preventing vascular differentiation from the existing procambium. Therefore, these inhibitors seem to affect venation by disrupting the development of procambial patterns. The *EMB30/GN* gene encodes a guanine nucleotide exchange factor (GEF) on adenosine diphosphate (ADP)-ribosylation factor-GTPase (ARF–GEF), which is responsible for the

targeted recycling of PIN1 putative auxin efflux carrier. Consequently, the *EMB30/GN* gene is required for the maintenance of polar auxin transport (Shevell et al., 1994; Busch et al., 1996; Steinmann et al., 1999; Geldner et al., 2003), and mutations in this gene cause irregular and discontinuous venation, with the formation of clustered or scattered tracheary elements (Mayer et al., 1991; Mayer et al., 1993; Koizumi et al., 2000).

The importance of auxin in the generation of venation has also been demonstrated in auxin-response mutants. *Arabidopsis* mutants defective in perceiving auxin, such as *auxin resistant 6* [*axr6* (Hobbie et al., 2000; Hellmann et al., 2003)] and *bodenlos* (Hamann et al., 1999; Hamann et al., 2002), exhibit severely reduced vascular networks. In the *monopteros* (*mp*) mutant, which is defective in an auxin-response transcription factor (IAA24/ARF5), marginal leaf veins are missing or interrupted and the capacity for polar auxin transport is reduced (Mayer et al., 1991; Berleth and Jürgens, 1993; Przemeczek et al., 1996; Mattsson et al., 2003). Recently, using auxin-inducible promoters fused to the β -glucuronidase (*GUS*) reporter gene, three laboratories have visualized auxin response patterns. Results suggest the preferential accumulation of auxin in the pre-procambial cells of young leaves (Avsian-Kretschmer et al., 2002; Aloni et al., 2003; Mattsson et al., 2003). This is additional evidence for the involvement of auxin in the generation of venation.

Based on physiological analyses of experimentally induced vascular differentiation, Sachs (Sachs, 1991) proposed the 'auxin signal flow canalization hypothesis', which presents the following scenario for the spatial regulation of vascular differentiation. Auxin flow, starting initially with diffusion, induces the formation of the polar auxin transport cell system. This, in turn, promotes auxin transport and leads to canalization of the auxin flow along a narrow file of cells. This continuous file of cells differentiates into a strand of procambial cells, and eventually into vascular cells. The auxin canalization hypothesis is consistent with the aforementioned data relating auxin and venation, and is in good agreement with currently accumulating data on PIN proteins (Benková et al., 2003). Hence, the auxin canalization hypothesis might provide a theoretical framework with which to understand the basic mechanism of venation generation.

However, at the molecular level, the auxin canalization hypothesis contains many unresolved problems. How are the sources and sinks of auxin that are necessary for the initial flow of auxin located in specific positions? How does auxin flow rearrange the auxin polar transport system to be canalized? How does the canalized auxin flow induce procambial and vascular differentiation? The possibility also remains that some unknown mechanisms act co-operatively with the auxin canalization mechanism to generate venation.

According to the assumptions of the auxin canalization hypothesis, a continuous flow of auxin is a prerequisite for vascular patterning. Therefore, the overall architecture of the vascular pattern is expected to be more sensitive to genetic lesions than is vascular continuity. A number of *Arabidopsis* mutants, including *lop1/tornado1* (Carland and McHale, 1996), *vascular network defective1 to 6* [*van1-6* (Koizumi et al., 2000)], *scarface*, [*sfc* (Deyholos et al., 2000)] and *cotyledon vein pattern 1* and *2* [*cvp1*, *cvp2* (Carland et al., 1999; Carland et al., 2002)], have discontinuous secondary

vascular strands in their cotyledons and leaves. Interestingly and unexpectedly, in most of these mutants, although the vein networks are fragmented, the overall architecture is normal. The high frequency of venation mutants of this type cannot be explained simply by the auxin canalization hypothesis.

To elucidate the molecular basis of the spatial regulation of leaf vascular development, we have identified the causal gene of the *van3* mutant, which of the six *van* mutants shows the most specific and restricted effect on the continuity of procambial cells. The *VAN3* gene encodes a unique type of ARF-guanosine triphosphatase (GTPase)-activating protein (GAP), which is located in the trans-Golgi network (TGN). Phenotypic analysis of the *van3* mutant suggests that the *VAN3* ARF-GAP may play an important role in the vesicle transport responsible for the auxin signaling that is required for vascular differentiation.

Materials and methods

Plant strains and growth conditions

The Landsberg *erecta* (*Ler*) strain of *Arabidopsis thaliana* (L.) Heynh was used as the wild-type, and the *van3* (*Ler*) mutant was used in this study unless otherwise indicated. Mutants *pin1-3* (*Ler*) (Bennette et al., 1995), *emb30-7/gn* (*Ler*) (Koizumi et al., 2000), and *mpT370* (*Ler*) (Berleth and Jürgens, 1993) were used for double mutant analyses. Surface-sterilized seeds were plated on growth medium (GM) containing Murashige and Skoog basal salts, 1.0% (w/v) sucrose, 0.05% (w/v) Mes (pH 5.7) and 0.3% (w/v) Phytigel (Sigma-Aldrich). Seeds were then transferred to a growth room at 22°C under continuous white light (20-50 $\mu\text{mol}/\text{m}^2/\text{second}$).

Double mutant analyses

To generate double mutants of *van3* with the *pin1-3*, *emb30-7/gn* or *mp^{T370}*, plants heterozygous for *van3* were crossed with plants heterozygous for *pin1-3*, *emb30-7/gn* or *mp^{T370}*. Double mutants were identified within F₂ families that segregated for each single mutant, and were distinguished by the presence of the distinct morphological features characteristic of each parental mutant phenotype. Furthermore, the genotypes of *van3 emb30-7/gn* and *van3 mp* double mutants were confirmed by cleaved amplified polymorphic sequences (CAPS; data not shown). In the double mutant combinations of *van3* with *pin1*, and *van3* with *emb30-7/gn*, mutants from each combination segregated at ratios of about 9:3:3:1 (WT:*van3:pin1:van3 pin1* = 348:112:105:30, χ^2 0.500, $<P < 0.750$; WT:*van3:emb30-7/gn:van3 emb30-7/gn* = 339:89:93:30, χ^2 0.050, $<P < 0.100$; WT:*van3:mp:van3 mp* = 236:76:90:28, χ^2 0.143, $<P < 0.504$).

Chemicals

Naphthalene acetic acid (NAA; Sigma-Aldrich), *N*-1-naphthylphthalamic acid (NPA; Tokyo Kasei Kogyo, Tokyo, Japan), and brefeldin A (BFA; Sigma-Aldrich) were used as 100 mM stock solutions in dimethylsulfoxide (DMSO). These chemicals were added to the autoclaved medium.

Histochemical staining for GUS

For the analysis of *DR5::GUS* expression in *van3* mutants, the *van3* mutation was introduced into *DR5::GUS* transgenic plants by crossing. For histochemical analysis, GUS staining was performed as described by Koizumi et al. (Koizumi et al., 2000), except that samples were incubated in the GUS substrate solution for 2 hours. Fixed samples were dehydrated through a graded ethanol series and embedded in Technovit 7100 resin (Heraeus Kulzer, Germany). Sections (6 μm) were cut with a microtome and observed under a light microscope equipped with Nomarski optics. The density of GUS-positive spots was measured using first-node leaves of 7-day-old

seedlings. Leaves of about the same length (850–1,100 μm) were used. Spots and leaf area measurements were made after the specimens were photographed. For the analysis of the auxin response, cotyledons of 7-day-old seedlings and first-node leaves of 11-day-old plants were excised at the center. They were then incubated in 1 ml of liquid GM containing NAA for 6 hours, with subsequent histochemical detection.

RT-PCR analysis

Total RNA was isolated as described previously (Sawa et al., 2002), and RT-PCR analysis to quantify the expression of auxin-inducible genes was performed according to the instructions for the Ready-To-Go RT-PCR Beads (Amersham Pharmacia Biotech), using a set of primers specific to the *VAN3* gene: 5'-GCTCCTCTCACATA-CAAATT-3' (forward), and 5'-GCTTTCTGGACAGAGAAATAGC-3' (reverse). To detect the levels of control transcripts, we used *ACT2* primers 5'-CTTCCTTGACTGCTTCTC-3' (forward) and 5'-TCA-TCGTCACCACCTTCA-3' (reverse).

Positional cloning of *VAN3*

The *VAN3* locus was mapped between the *RC11B* and *nga151* markers on chromosome 5 (Koizumi et al., 2000). A number of new simple sequence length polymorphism (SSLP) and CAPS markers between *RC11B* and *nga151* markers were developed from data obtained from the TAIR database and Cereon Genomics (data not shown). In the F_2 generation produced from crosses between *van3* heterozygotes (*Ler*) and Columbia, recombinants between the *VAN3* locus and the new SSLP and CAPS loci were scored. From 1034 chromosomes, 784 were analyzed and the *VAN3* locus was identified in the 89 kb region between the T31B5c and T22N19c markers. This corresponds to two adjoining bacterial artificial chromosome (BAC) clones including 22 putative genes in the interval between the T31B5c and T22N19c markers (Arabidopsis Genome Initiative). These were PCR-amplified from the *Ler* strain and *van3*, and completely sequenced using the BigDye Terminator Cycle Sequencing Kit on an ABI PRISM 370 Genetic Analyzer. Among these putative genes, only the T31B5.120 (*At5g13300*) gene contained a mutation in a putative exon. An 8.6 kb *XbaI-SpeI* genomic DNA fragment that included the 1.1 kb upstream region of this gene and the 1.1 kb downstream region (position 51627–60181 of T31B5 BAC) was cloned into the vector pGreen 0179. The clone was introduced into *Agrobacterium tumefaciens* strain C58 and transformed into plants carrying the heterozygous *van3* mutation (*van3-1/VAN3*) using the floral dip method. After hygromycin selection, T_2 seeds were collected from individual T_1 plants and T_2 lines were constructed. All T_2 line seeds were grown with hygromycin and the segregation of resistance was examined. In the T_2 line, plants presumed to carry single copies of T-DNA and a heterozygous *van3* mutation segregated at ratios close to 15:1 (WT: *van3* = 197:10, χ^2 0.250, $P < 0.500$). These results led us to conclude that the *VAN3* gene corresponds to T31B5.120.

Subcellular localization of *VAN3*

Full-length *VAN3* cDNA was isolated by RT-PCR from the *A. thaliana* Columbia ecotype, and an *XhoI/NcoI* restriction site was introduced at both ends. The fragment was translationally fused to the N terminus of Venus yellow fluorescent protein. The chimeric gene was subcloned under the control of the cauliflower mosaic virus 35S promoter and the Nos terminator. 35S::ARA7-GFP (Ueda et al., 2001), 35S::ARA6-GFP (Ueda et al., 2001), 35S::HDEL-GFP (Takeuchi et al., 2000), 35S::SYP31 (Takeuchi et al., 2002), 35S::VAMP727-GFP, and 35S::SYP41-GFP were used as intracellular markers of early endosomes, late endosomes, ER, cis-Golgi, early endosomes and TNG, respectively. Double transient expression of 35::VAN3-Venus and of intracellular markers in the protoplasts of cultured *Arabidopsis* cells were analyzed as described by Ueda et al. (Ueda et al., 2001). Protoplasts from *gnom* mutant cells were prepared as described by Geldner et al. (Geldner et al., 2003).

Fluorescence was observed by confocal laser microscopy (LSM510 META, Carl Zeiss).

ARF-GAP assays

Myristoylated yeast ARF1p (myr-ARF1p) was purified from *Escherichia coli* co-transfected with expression vectors for ARF1p and yeast *N*-myristoyltransferase, as described previously (Randazzo et al., 1994; Randazzo et al., 1995). ARF-GAP activity was determined by an in vitro assay that measured a single round of GTP hydrolysis in recombinant myr-ARF1p (Makler et al., 1995; Huber et al., 2001; Huber et al., 2002). Myr-ARF1p (5 μM) was first loaded with 5 μM [α - ^{32}P]GTP in ARF-loading buffer [25 mM Hepes (pH 7.5), 1 mM dithiothreitol, 2 mM ethylenediaminetetraacetic acid (EDTA), 1 mM MgCl_2 , 10 mM ATP, 3 mM dimyristoyl phosphatidylcholine and 0.1% sodium cholate]. The reaction was stopped with the addition of MgCl_2 at a final concentration of 3 mM, and a GAP assay was performed at 30°C in 50 mM Hepes (pH 7.5), 4 mM MgCl_2 , 10 mM ATP, and recombinant VAN3. The reaction was initiated with the addition of 1 μM [α - ^{32}P]GTP-loaded ARF1p, and stopped with the addition of 250 mM EDTA. The medium was then placed on ice. Nucleotides were separated by thin-layer chromatography on poly(ethyleneimine)-cellulose sheets developed with 1 M LiCl and 1 M HCOOH. The sheets were dried, autoradiographed on an imaging plate, and quantitatively analyzed with a BioImaging Analyzer (BAS 2500, Fuji Photo Film). In the absence of ARF1p, VAN3 showed no GTP hydrolysis activity (data not shown).

Fat western blotting

Phospholipids (Sigma-Aldrich) were prepared in chloroform as stock solutions at concentrations of 1 mg/ml. Solutions (10 μl) containing 0.5 or 1 μg of lipid were spotted individually onto nitrocellulose. The membrane and lipids were dried at room temperature for 1 hour, and the nitrocellulose was incubated with 3% (w/v) fatty-acid-free bovine serum albumin (isolated by cold ethanol precipitation; Sigma-Aldrich A-6003) in Tris-buffered saline-Tween 20 (TBST) solution [10 mM Tris (pH 8.0), 140 mM NaCl, 0.1% (v/v) Tween 20] for 1 hour. The membrane was then placed in a solution containing GST-tagged recombinant type V VAN3 fusion protein diluted in TBST (0.5 $\mu\text{g}/\text{ml}$) and incubated at 4°C overnight with shaking. The nitrocellulose was then washed with TBST three times for 10 minutes each and incubated with anti-VAN3 antibody diluted 1:2000 in TBST for 1 hour at room temperature. The membrane was then washed three times for 10 minutes each in TBST at room temperature and incubated for 1 hour at room temperature with goat anti-rabbit-IgG antibody conjugated with horseradish peroxidase, diluted 1:10000 in TBST. The nitrocellulose was washed again three times in TBST for 10 minutes each and incubated for 5 minutes in a 1:1 mixture of peroxidase substrate and luminol/enhancer (Pierce) for subsequent chemiluminescence detection. The nitrocellulose was exposed to Hyperfilm ECL (Amersham Pharmacia Biotech) for 0.5–1 minute. The anti-VAN3 antibody was raised against a synthetic peptide encoded between the BAR and PH domains, EKMQEYKRQVDRESR, injected into a rabbit (Sawady Technology, Tokyo, Japan).

Yeast two-hybrid analysis

A two-hybrid analysis was performed using the Matchmaker Two-Hybrid System 3 (Clontech); pGADT7 was used for GAL4 AD and pGBKT7 was used for GAL4 DNA-BD. A standard complete yeast extract-peptone-dextrose medium was used for cell growth, and synthetic dextrose medium was used as the selective medium to which tryptophan, leucine, adenine and histidine were added as needed to final concentrations of 200 mg/l, 1 g/l, 200 mg/l and 200 mg/l, respectively. Protein-protein interactions were detected by yeast (strain AH109) viability on agar plates without adenine or histidine. Full-length *VAN3* cDNA and seven types of truncated *VAN3* cDNAs

(Fig. 5D) were amplified using PCR, confirmed by sequencing, and cloned into pGADT7 and/or pGBKT7, as shown in Fig. 5D.

Accession number

The ORF of the *VAN3* gene has been submitted to GenBank under accession number AB194395.

Results

Genetic interaction between *VAN3* and *PIN1*, *EMB30/GN* and *MP*

The cotyledon of *Arabidopsis* has a very simple vein pattern: one midvein and three or four lateral veins (Fig. 1A). Taking this pattern as an index, we isolated *van1* to *van7* mutants (Koizumi et al., 2000). The *van3* mutant has a discontinuous vascular network in cotyledons, with no significant effect on the overall architecture of the vascular pattern, and the leaves did not show obvious variability in their architecture within and between plants (Fig. 1B). In *van3* rosette leaves, minor veins also show severe discontinuity (Fig. 1C,D), which varies from leaf to leaf.

To understand the function of *VAN3* in vascular pattern formation, we first examined the relationship between *VAN3* and auxin by generating the double mutants *van3 pin1*, *van3 emb30-7* and *van3 mp*. For this purpose, we used the phenotypes of weak alleles to detect genetic interaction easily. About half the *pin1-3* seedlings produced fused cotyledons,

and the midvein was occasionally furcated (Fig. 1E) (Aida et al., 2002). In the *van3 pin1-3* double mutant, about half the seedlings produced fused cotyledons, and the cotyledon contained a single or furcated midvein (Fig. 1F). The lateral veins of the cotyledons were fragmented in the *van3 pin1-3* double mutant. This additive phenotype suggests that *VAN3* and *PIN1* could be independently responsible for vascular formation.

About half the *emb30-7* seedlings produced fused cotyledons similar to those of the *pin1-3* mutant, and the *emb30-7* cotyledons had irregularly concentrated vascular tissues (Fig. 1G) (Koizumi et al., 2000). In the *van3 emb30-7* double mutant, about half the seedlings produced fused cotyledons that contained a single midvein and fragmented lateral veins (Fig. 1H). Lateral veins of the *van3 emb30-7* cotyledons were more fragmented than those of *emb30-7*, and no concentrated vascular tissues were observed. The architecture of the venation was similar to that of the *van3* mutant. Rosette leaves of the *emb30-7* mutant have concentrated vascular tissues with an increased number of trachery elements (TEs). This phenotype was also observed in rosette leaves treated with an auxin transport inhibitor (Fig. 1I, Fig. 2A-D). The *van3 emb30-7* double mutant produced rosette leaves similar to those of the *van3* mutant (Fig. 1D,J), suggesting that the concentrated vascular pattern induced in the *emb30* mutant is suppressed by the *van3* mutation.

The *MP* gene encodes an auxin response factor that mediates auxin signaling, *IAA24/ARF5*. To examine the genetic interaction between the *van3* and *mp* mutations, we generated *van3 mp* double mutants. The *mp* mutants usually produce a secondary vein in the cotyledons (Fig. 1K), whereas the double mutants did not. In an extreme case, no midvein was formed (Fig. 1L). These results suggest that the *VAN3* mutation enhances the effects of the *MP* mutation.

VAN3 and the polar auxin transport system do not act in the same pathway in vascular pattern formation

To further investigate the relationship between *VAN3* function and polar auxin transport in vein pattern formation, we treated the *van3* plants with the auxin transport inhibitor, N-1-naphthylphthalamic acid (NPA). In the first-node leaves of wild-type plants, vascular differentiation was enhanced along the entire lamina margin, and the marginal vascular tissues were connected to the central vascular tissues with an increased number of non-branched vascular tissues (Fig. 2A-D). These effects depended on NPA concentration (Fig. 2A-D) (Mattsson et al., 1999; Mattsson et al., 2003; Sieburth, 1999). In the first-node leaves of the *van3* mutant grown with NPA, vascular formation was enhanced and the vasculature was

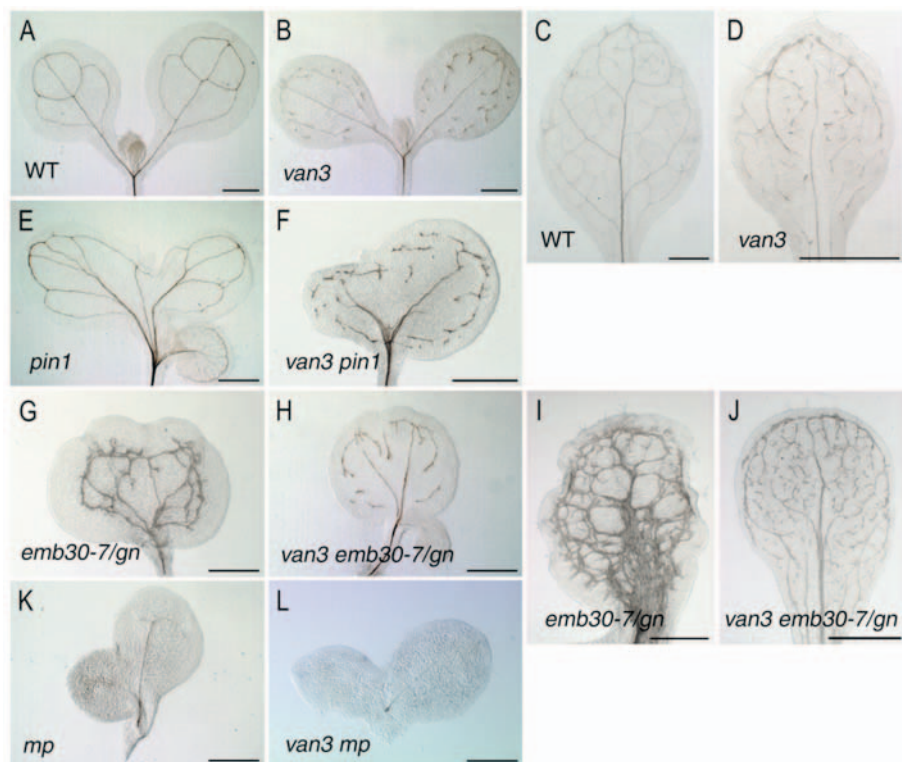


Fig. 1. Vein patterns in *van3*-related mutants. Vein patterns of the cotyledons of 7-day-old seedlings (A,B,E,F,G,H,K,L) and in first-node leaves of 11-day-old plants (C,D,I,J). (A) Wild-type. (B) *van3* mutant. (C) Wild-type. (D) *van3* mutant. (E) *pin1-3* mutant. (F) *van3 pin1-3* double mutant. (G) *emb30-7/gn* mutant. (H) *van3 emb30-7/gn* double mutant. (I) *emb30-7/gn* mutant. (J) *van3 emb30-7/gn* double mutant. (K) *mpT370* mutant. (L) *van3 mpT370* double mutant. Genotypes were identified by CAPS analysis using root DNA. Scale bars: (A-L) 1 mm.

and excess vascular formation seemed to be suppressed (Fig. 2M–P).

Minor veins are discontinuously formed with auxin accumulation, and the auxin response is reduced in the *van3* mutant

To understand the effect of the *VAN3* mutation on auxin distribution, we examined the expression pattern of the *DR5::GUS* construct as a marker of auxin accumulation. In the first-node leaves of wild-type seedlings, GUS staining was observed as a dotted pattern in the hydathodes and developing minor veins (Fig. 3A–E). Each dot represented a cell or a few cells, and their shapes varied from round and oval to elongated (Fig. 3E). In the *van3* mutant, the GUS staining pattern in developing leaves was similar to that of the wild-type (Fig. 3F–J). However, the number of GUS-expressing spots was significantly reduced [wild type: $46.7 \pm 3.8/\text{mm}^2$ of leaf ($n=24$); *van3*: $5.8 \pm 2.3/\text{mm}^2$ of leaf ($n=18$); values represent means \pm s.e.m.]. These results suggest a reduction in the number of auxin-accumulating cells and/or a reduction in auxin sensitivity.

To investigate the role of *VAN3* in the auxin response, we examined the expression pattern of the *DR5::GUS* construct in the *van3* mutant treated with auxin. In the cotyledons of wild-type seedlings, expression of the ectopic *DR5::GUS* marker was induced by exogenously applied auxin (Fig. 3K–M, Q–S), whereas *DR5::GUS* expression in the *van3* mutant was less sensitive to auxin (Fig. 3N–P, T–V). We also examined the auxin response in the *van3* roots and hypocotyls by analyzing auxin-induced *DR5* expression, the gravitropic response, callus formation and the inhibition of root elongation, as described by Geldner et al. (Geldner et al., 2004), Willemsen et al. (Willemsen et al., 2003) and Hobbie et al. (Hobbie et al., 2000), respectively. The responses were almost the same as those of wild-type plants (data not shown). These results suggest that the *VAN3* gene may be responsible for the auxin response, at least in the cotyledons and rosette leaves.

VAN3 encodes an ARF–GAP

To gain further insight into the molecular nature of the *VAN3* gene, we isolated it using a positional cloning method. The *VAN3* locus was mapped to chromosome 5, in the 89 kb region between molecular markers T31B5c and T22N19c (Fig. 4A). We sequenced the genomic DNA of the *Ler* strain and the *van3-1* mutant spanning 22 annotated open reading frames (ORFs) identified in this region, and found a point mutation only in ORF T31B5.120 (*At5g13300*). An 8.6 kb wild-type genomic fragment that includes 1.1 kb upstream from the putative transcription start site and 1.1 kb downstream from the putative transcription termination site of this ORF complemented the discontinuous vascular phenotype of the *van3* mutant (detailed in Materials and methods). We identified ORF *At5g13300* as the *VAN3* gene.

The *VAN3* gene encodes a protein of 827 amino acids, and the Trp at codon 356 is changed to a stop codon in the *van3-1* mutant (Fig. 4B). The SMART system (<http://smart.embl-heidelberg.de/>) predicts the *VAN3* protein to have four domains: a BAR (BIN/amphiphysin/RVS) domain, a pleckstrin homology (PH) domain, an ARF–GAP domain and three ankyrin (ANK) repeats. These domains are located at residues 11–218, 293–432, 501–643 and 728–826, respectively (Fig. 4B).

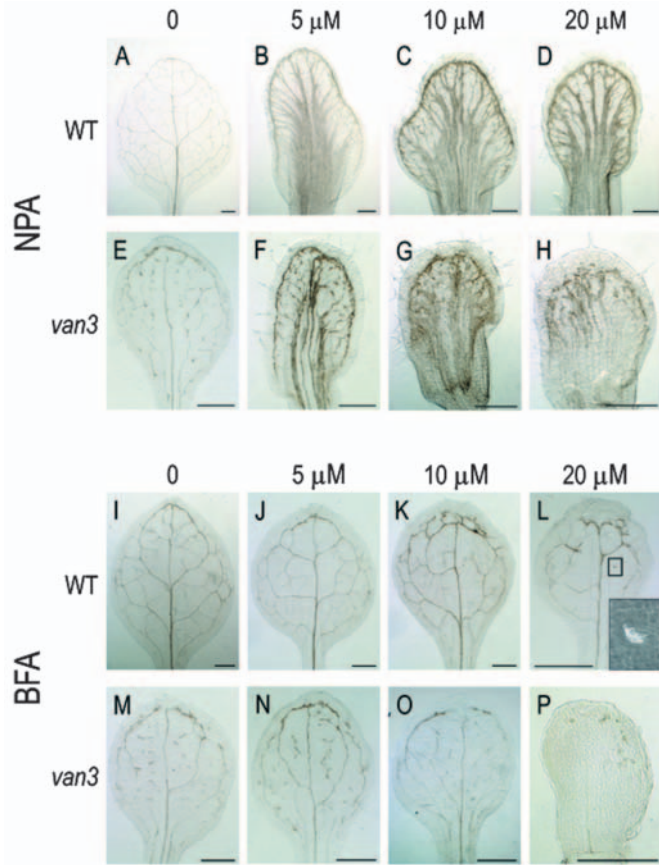


Fig. 2. Effects of NPA and BFA on vein patterning. Vein patterns of first-node leaves of the wild-type (A–D, I–L) and the *van3* mutant (E–H, M–P) grown for 11 days on agar medium containing NPA (A–H) or BFA (I–P). Mock-treated leaves are shown in A, E, I, M. Chemicals were applied at concentrations of 5 μM (B, F, J, N), 10 μM (C, G, K, O), or 20 μM (D, H, L, P). Inset in L is a close-up of a trachery element island under Nomarski optics. Scale bars: (A–P), 500 μm .

fragmented. However, the overall pattern was the same as that of wild-type plants treated with NPA (Fig. 2E–H, most obvious in F). Similar effects were observed in the *van3* leaves treated with 2,3,5-triiodobenzoic acid (TIBA) (data not shown). These results suggest that the effects of the auxin transport inhibitor and the *VAN3* mutation are additive in the formation of the venation pattern in the *Arabidopsis* leaf. Thereafter, *VAN3* probably acts independently of polar auxin transport in vascular pattern formation, although we cannot exclude the possibility that *VAN3* functions in the polar auxin transport system.

Brefeldin A (BFA) prevents the polarized transport of PIN1 protein to the plasma membrane by inhibiting the activation of GNOM ARF–GEF (Geldner et al., 2001). In wild-type plants grown with BFA, the size of the first-node leaf was reduced, and the vein pattern was simplified in a BFA-concentration-dependent manner (Fig. 2I–L). TEs were also excessively differentiated in the upper part of the leaf margin, but not in the central region treated with BFA (Fig. 2K, L). After treatment with 20 μM BFA, tertiary veins occasionally developed discontinuously (Fig. 2L). In the *van3* mutant treated with BFA, secondary and tertiary veins were missing

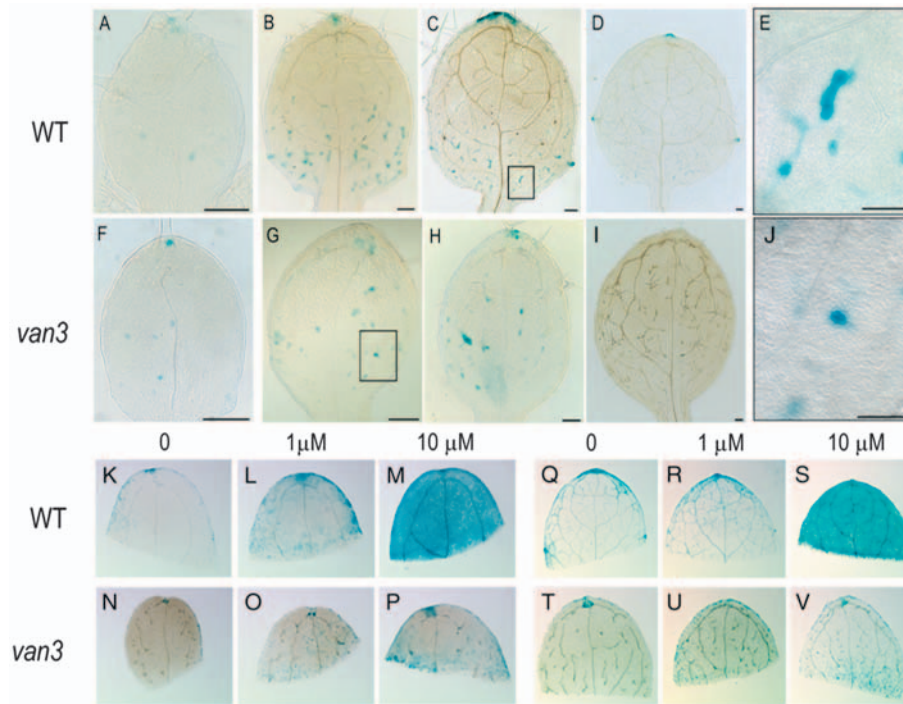


Fig. 3. *DR5::GUS* expression patterns. *DR5* expression patterns in the developing first-node leaves of the wild-type (A–D) and *van3* mutant (F–I). Samples were harvested from 6- (A,F), 7- (B,G), 8- (C,H) and 10-day-old (D,I) seedlings. E and J show magnified views of the boxed regions in C and G, respectively. *DR5::GUS* expression pattern in the excised cotyledons (K–P) and first-node leaves (Q–V) treated with NAA. The wild-type (K–M,Q–S) and *van3* mutant (N–P,T–V) samples were exposed to NAA for 1 hour: mock-treated controls (K,N,Q,T); 1 μ M NAA (L,O,R,U), 10 μ M NAA (M,P,S,V). Scale bars: 100 μ m.

The BAR domain is expected to mediate protein–protein interactions (Navarro et al., 1997), whereas the PH domain is known to mediate protein–lipid interactions (Harlan et al., 1994). The ARF–GAP domain contains a consensus zinc finger motif and functions in the stimulation of GTP hydrolysis (Cukierman et al., 1995). ANK repeats are involved in protein–protein interactions and associate to form a higher-order structure. A homology search using the DNA Data Bank of Japan revealed significant sequence similarity between the putative VAN3 protein and the human ARF–GAPs with coiled-coil domains, ANK repeats and PH domains, ACAP1 (32% identical) and ACAP2 (33% identical) (Jackson et al., 2000). VAN3 has the same domain structure as ACAP1 and ACAP2 (Fig. 4B). The ARF–GAP domain is highly conserved between VAN3 and the ACAPs (Fig. 4C), suggesting that the VAN3 protein may function as an ARF–GAP. Many genes showing significant sequence similarities to the *VAN3* gene were found in *Arabidopsis thaliana*, *Oryza sativa*, *Anopheles gambiae*, *Mus musculus*, *Fugu rubripes*, *Drosophila melanogaster*, *Dictyostelium discoideum* and *Caenorhabditis elegans*. In the *Arabidopsis* genome, three genes, *At5g61980*, *At1g10870* and *At1g60860*, show significant sequence similarities to the *VAN3* gene. The deduced amino acid sequences of these homologs are 47–62% identical to that of VAN3, and the domain structures of these proteins are the same as that of VAN3 (Fig. 4B). In particular, sequences of the BAR domains are strongly conserved between VAN3 and these predicted proteins (Fig. 4C).

***VAN3* expression is induced by auxin and is self-regulated**

Next, we examined the effects of auxin on *VAN3* expression in the cotyledons. We used RT–PCR because *VAN3* and *VAN3* homologs have high sequence similarity and probes specific to the 5′- and 3′-UTR regions of these genes did not give clear signals on northern analysis. The intensity of the PCR band corresponding to the *VAN3* gene increased significantly with auxin treatment of wild-type cotyledons (Fig. 4D). In contrast, *VAN3* gene expression level seems to be reduced by auxin treatment in the *van3* mutant (Fig. 4D). This indicates that *VAN3* expression is upregulated by auxin, and its auxin-dependent induction may be positively regulated by VAN3 itself.

***VAN3* protein has ARF–GAP activity**

We examined the ARF–GAP activity of the VAN3 protein using an in vitro ARF–GAP assay. A glutathione S-transferase (GST) fusion protein and type V VAN3 protein that lacked the BAR domain (Fig. 5D) were expressed in *E. coli* and purified. The hydrolysis of GTP on recombinant yeast Arf1p was measured with or without recombinant VAN3 protein. VAN3 protein induced GTP hydrolysis on yeast Arf1p in a concentration- and incubation-time-dependent manner (Fig. 5A,B). These results indicate that VAN3 protein functions as an ARF–GAP that regulates ARF cycling between the active ARF–GTP form and the inactive ARF–guanosine diphosphate (GDP) form in the vesicle transport pathway.

Recombinant VAN3 protein binds to PI-4-P

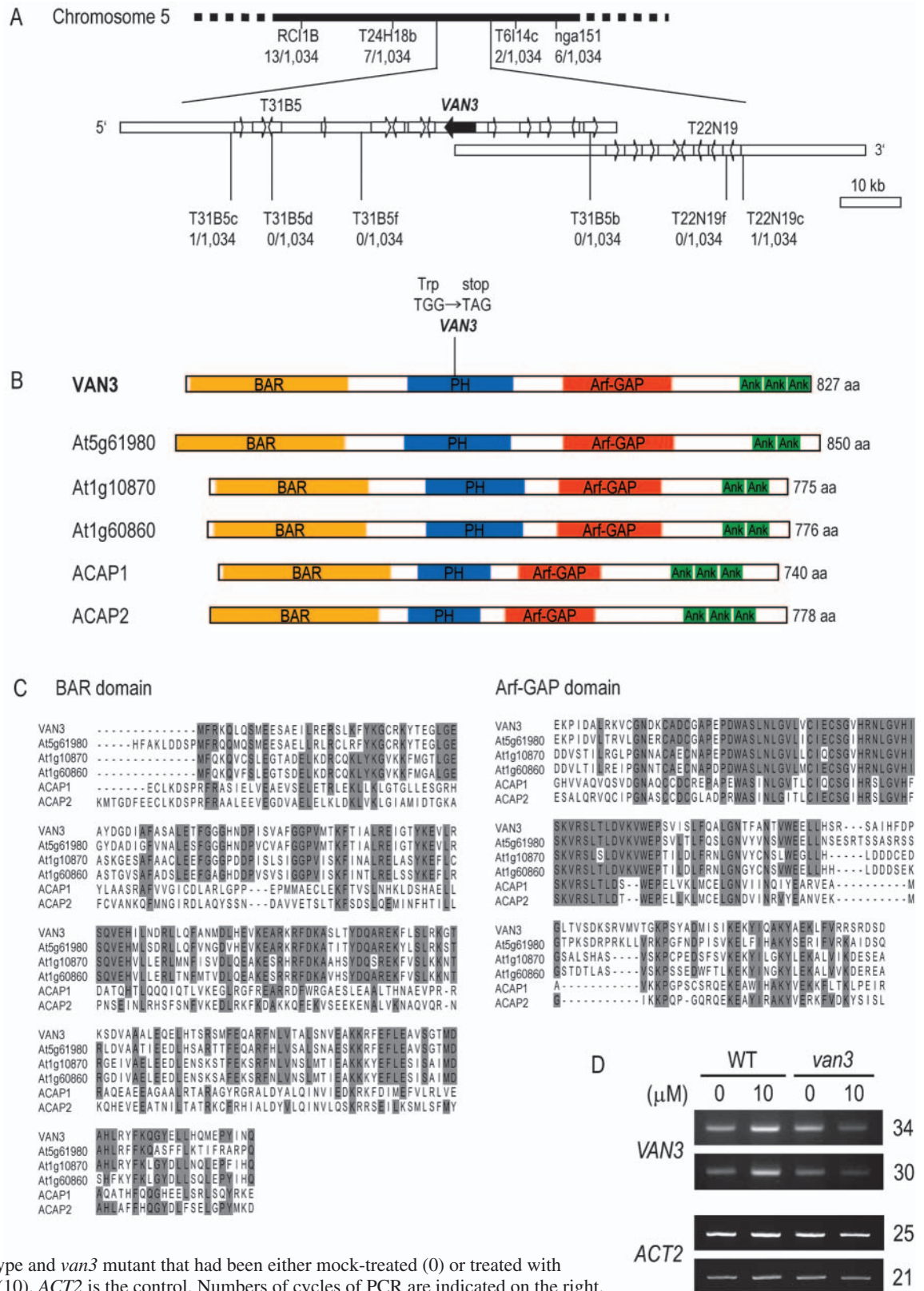
The PH domain is found in a wide variety of signaling proteins and binds to phosphoinositides (Harlan et al., 1994). Furthermore, human ACAPs, which have significant sequence similarity to VAN3, are known to bind the lipid phosphatidylinositol 4,5-bisphosphate [PtdIns(4,5) P_2]. To determine whether the VAN3 protein binds to a lipid, we purified recombinant type V VAN3 protein (Fig. 5D) using affinity chromatography (data not shown). The ability of the recombinant VAN3 protein to bind different phospholipids was examined using fat western blotting, developed by Stevenson et al. (Stevenson et al., 1998). Fig. 5C shows the results of fat western blotting probed with recombinant VAN3 protein. VAN3 bound to phosphatidylinositol (PtdIns), phosphatidylinositol 4-monophosphate (PtdIns4P) and PtdIns(4,5) P_2 , but not to phosphatidic acid (PA), phosphatidylcholine (PC), or phosphatidylethanolamine (PE). VAN3 bound to PtdIns4P with higher affinity than to PtdIns or PtdIns(4,5) P_2 . Recombinant GST protein did not bind to any of the lipids tested (data not shown).

VAN3 forms a homodimer

The BAR domain is known to mediate protein-protein interactions (Navarro et al., 1997). To determine whether the VAN3 protein forms a homodimer through the BAR domain,

we performed yeast two-hybrid analyses. Eight types of VAN3 cDNA fragments were translationally fused to the GAL4 activation domain (AD) and/or GAL4 DNA-binding domain (DNA-BD) (Fig. 5D). Types I-VII were composed of the BAR

Fig. 4. Molecular cloning and expression of VAN3. (A) VAN3 was isolated by positional cloning and mapped to the 89 kb region between the T31B5c and T22N19c markers, which corresponds to two adjoining BAC clones, T31B5 and T22N19. Numbers below the molecular markers indicate the recombination frequency between the marker and the VAN3 locus (recombinant chromosomes/analyzed chromosomes). Black lines and outlines show the VAN3 gene (*At5g13300*) and putative genes in this region, respectively. (B) Structure of the VAN3 protein and its homologs from the predicted proteins of *Arabidopsis* and humans. The VAN3 gene encodes an ARF-GTPase-activating protein (ARF-GAP) that includes BAR, PH, ARF-GAP and three-ANK-repeat domains. The mutation in the *van3* mutant (TGG [Trp356] to TAG [stop]) is indicated. (C) Comparison of BAR and ARF-GAP domains. Conserved amino acid residues are highlighted by grey boxes. (D) Semi-quantitative RT-PCR analysis of the expression of the VAN3 gene in the wild-type and *van3* mutant. RNA was isolated from 7-day-old seedling cotyledons of the wild-type and *van3* mutant that had been either mock-treated (0) or treated with 10 μM NAA for 1 hour (10). ACT2 is the control. Numbers of cycles of PCR are indicated on the right.



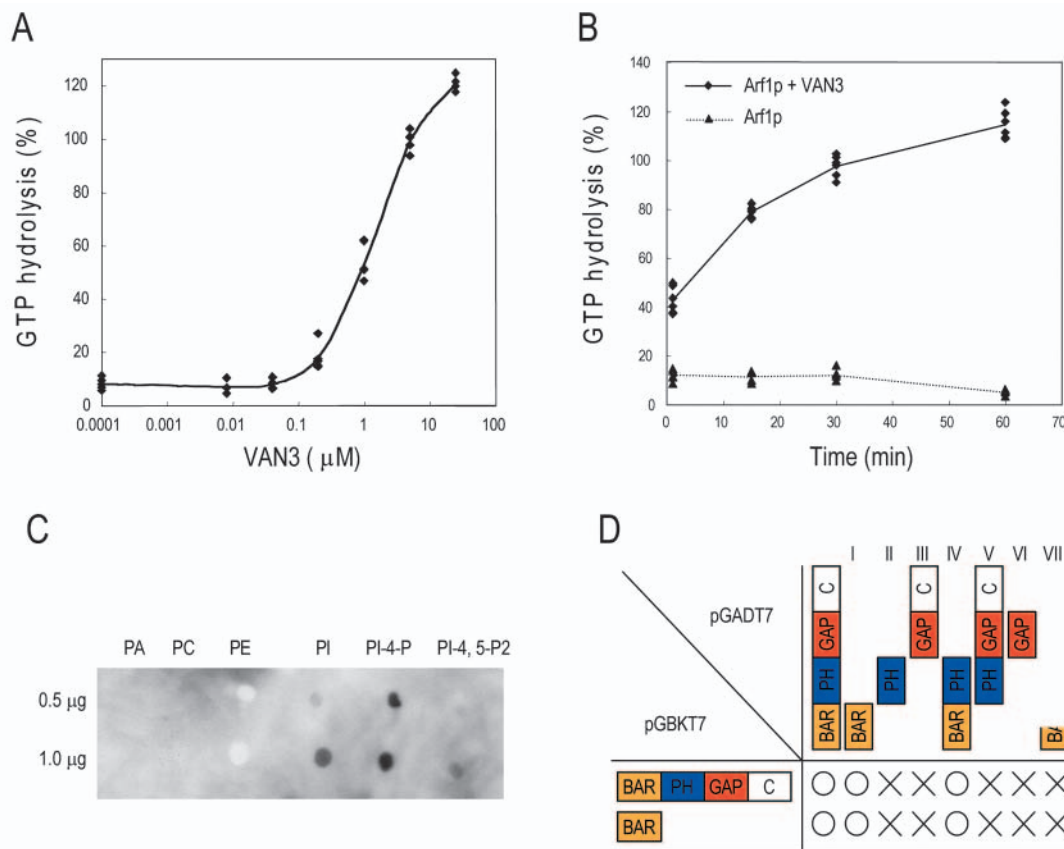


Fig. 5. Characterization of the VAN3 protein. (A,B) ARF-GAP activity of recombinant VAN3 proteins in vitro. GAP activity was assessed by the hydrolysis of GTP bound to the yeast ARF1 protein. (A) Concentration dependence of VAN3. Recombinant VAN3 protein was serially diluted, and incubated with 1 μ M [α - 32 P]GTP-loaded ARF protein at 30°C for 10 minutes. (B) Time-course of ARF-GAP activity of VAN3. Recombinant VAN3 (1 μ M) was incubated with 1 μ M [α - 32 P]GTP-loaded ARF1 protein at 30°C. Aliquots were withdrawn at the indicated times. (C) Fat western blots of phospholipids probed with recombinant VAN3. Phospholipids are indicated above each blot, and the amount of lipid spotted onto the nitrocellulose is shown to the left of each row of lipid. The blot was incubated with 0.5 μ g/ml GST-tagged recombinant type V VAN3. PA, phosphatidic acid; PC, phosphatidylcholine; PE, phosphatidylethanolamine; PI, phosphatidylinositol; PI-4-P, phosphatidylinositol 4-monophosphate; PI-4,5-P2, phosphatidylinositol 4,5-bisphosphate. (D) Homodimerization of VAN3 through the BAR domain. Constructs including full-length VAN3 (FLVAN3) and seven types of truncated VAN3 were fused to GAL4 AD in pGADT7, and those containing FLVAN3 and type I VAN3 were fused to GAL4 DNA-BD in pGBKT7. Proteins are represented by bars; motifs or domains within proteins are indicated by different colors. Circles show protein-protein interactions. Crosses show no interaction.

domain (amino acids 17-221); the PH domain (amino acids 221-441); the GAP and C-terminal domains (amino acids 439-827); the BAR and PH domains (amino acids 17-431); the PH-C terminal domain (amino acids 221-827); the GAP domain (439-706); and the truncated BAR domain (1-85), respectively. As shown in Fig. 5D, when the intact BAR domain was used in the yeast two-hybrid analysis, protein-protein interactions were detected. This indicates that the BAR domain is required and is sufficient for the formation of the VAN3 homodimer.

VAN3 localizes to a subpopulation of the TGN

ARF-GAP is a key component in vesicle formation for membrane transport, so VAN3 protein is expected to locate to an organelle involved in the secretory system. Furthermore, human ACAPs are located in endosomes. GNOM ARF-GEF, which is involved in vascular formation, is also considered to function in endosomes. However, VAN3 and ACAPs have different binding affinities for lipids, and VAN3 and GNOM seem to act differently in vascular pattern formation and have

different effects on auxin signaling. Therefore, we identified the subcellular location of VAN3 to better understand its function. VENUS (Nagai et al., 2002)-tagged VAN3 and green fluorescent protein (GFP)-tagged subcellular marker genes were co-introduced into *Arabidopsis* suspension-cultured cells (Fig. 6A), and their subcellular locations were observed with a confocal laser scanning microscope. The location of VAN3-Venus did not overlap with that of the endoplasmic reticulum (ER) marker HDEL-GFP (Takeuchi et al., 2000) or the Golgi body marker SYP31-GFP that marks the *cis* faces of Golgi stacks (Takeuchi et al., 2002). Furthermore, it also did not colocalize with the endosome marker, ARA6-GFP (Fig. 6B-D), ARA7-GFP and Vamp727-GFP (data not shown) (Ueda et al., 2001; Ueda et al., 2004). Nor did it colocalize with the lipophilic endocytic tracer FM4-64 (data not shown). We also examined the localization of VAN3-Venus in *gnom* suspension-cultured cells because cultured *gnom* cells contain abnormally enlarged endosomes that mediate the endosome-plasma membrane recycling of PIN1 (Geldner et

al., 2003). The structure of the organelle in which the VAN3-Venus protein was located was completely different from the enlarged organelle that was stained with the endosome marker ARA7-GFP in cultured *gnom* cells (Ueda et al., 2001; Geldner et al., 2003) (Fig. 6E,F). This indicates that VAN3 is not located in the endosomes in which GNOM functions. However, VAN3-Venus-positive compartments overlapped with those of the TGN marker, SYP41-GFP (Bassham et al., 2000; Uemura et al., 2004) (Fig. 6G-I). These results indicate that the VAN3 protein is located in the TGN. Interestingly, not all the TGN was positive for VAN3-Venus. This unique localization pattern suggests that the TGN is not uniform, but is functionally differentiated in plant cells.

Discussion

VAN3 encodes an AZAP-type ARF-GAP protein located in the TGN

We cloned the *VAN3* gene using a map-based strategy and showed that it encodes an AZAP-type ARF-GAP protein. The ARF-GAP proteins belong to several families that induce the hydrolysis of GTP bound to ARF. This affects membrane trafficking and actin remodeling (Donaldson and Klausner, 1994; Donaldson et al., 1995; Moss and Vaughan, 1995; Moss and Vaughan, 1998; Radhakrishna et al., 1999; Frank et al., 1998; Song et al., 1998; Franco et al., 1999). ARF-GAPs have been categorized into three groups: ARF-GAP1, Git and AZAP (Randazzo and Hirsch, 2004). VAN3 represents the first plant AZAP type of ARF-GAP protein to be functionally characterized, and plays a key role in morphogenesis. The AZAP-type ARF-GAP protein family is defined by several common structural motifs including PH, ARF-GAP and ANK-repeat domains. AZAP-type ARF-GAPs can be divided into four subtypes: ASAP, ACAP, ARAP and AGAP. The VAN3 protein has the same structural motifs as ACAP proteins (Fig. 4). Interestingly, only the ACAP subtype of the AZAP-type ARF-GAP proteins are encoded in the *Arabidopsis* genome. In animal cells, AZAP-type ARF-GAPs regulate processes such as cell migration, adhesion, and cell-cell contact. They are also important for development and wound healing (de Curtis, 2001). Given the participation of ARF proteins in regulating membrane traffic, one appealing hypothesis is that ARF-GAPs act as molecular devices that coordinate membrane traffic and cytoskeletal reorganization during cell motility (Randazzo et al., 2000; de Curtis, 2001; Turner et al., 2001). In contrast to the rapid progress in understanding AZAP-type ARF-GAPs in animals, there is no report of their

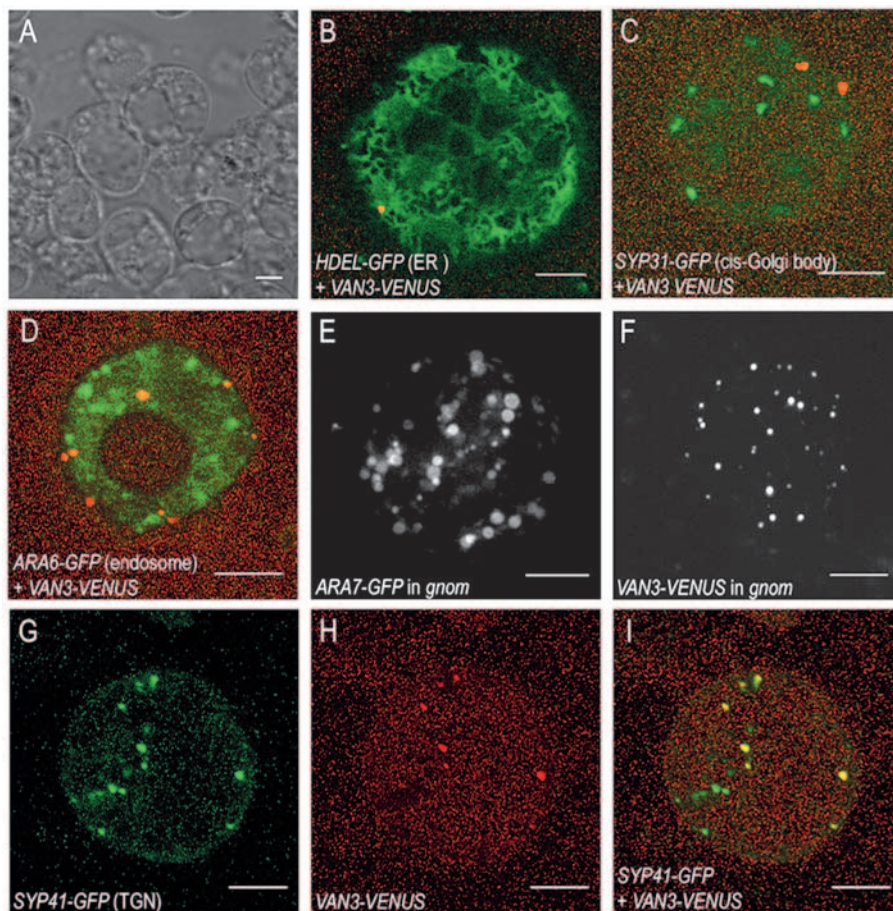


Fig. 6. Subcellular localization of VAN3. (A) *Arabidopsis* suspension-cultured cells. (B-D,G-I) Location of VAN3-Venus (red) and GFP-tagged subcellular marker genes (green). 35S-promoter-driven Venus-tagged VAN3 and GFP-tagged subcellular markers were co-introduced into protoplasts of *Arabidopsis* suspension-cultured cells. (B-D) Merged image of VAN3-Venus and the ER marker HDEL-GFP (B), the cis-Golgi marker SYP31-GFP (C), the endosome marker ARA6-GFP (D). (E) Location of ARA7-GFP in the *gnom* mutant cells. (F) VAN3-Venus in *gnom* mutant cells. (G-I) Localization of the TGN marker SYP41-GFP (G) and VAN3-Venus (H), and a merged image of G and H (I). E and F are projection images of serial confocal planes, A-D and G-I and single confocal slice images. Scale bars: (A-I) 5 μ m.

molecular mechanisms in plants. Therefore, this is the first report demonstrating ARF-GAP function in plant development.

Recombinant VAN3 protein showed ARF-GTPase-stimulating activity on yeast Arf1p, demonstrating that VAN3 can function as an ARF-GAP (Fig. 5A,B). The kind of ARF(s) activity that is regulated by VAN3 has yet to be identified. The six mammalian ARFs have been grouped into three classes: class I (ARF1-3), class II (ARF4 and ARF5) and the most distinctive group, class III (ARF6) (Moss and Vaughan, 1995; Jürgens and Geldner, 2002). ACAPs regulate ARF6-dependent membrane trafficking in animals (Jackson et al., 2000). In the *Arabidopsis* genome, six of nine putative ARF genes encode class I ARF proteins with 98-100% amino acid identity. The other three putative *Arabidopsis* ARFs diverge from animal and yeast ARFs and are difficult to classify into known groups. No clear evolutionarily conserved homolog of ARF6 is found in the *Arabidopsis* genome. Therefore, it would be interesting to

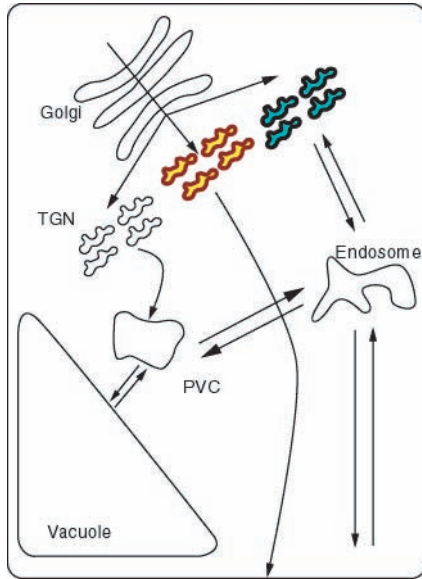


Fig. 7. Models of the functional differentiation of TGN in vesicle trafficking pathways. The TGN does not have a uniform function but is functionally differentiated into subpopulations that are specialized to transport to the plasma membranes (yellow), to endosomes (blue), or to prevacuolar compartments (PVC) (white). VAN3 is located in a subpopulation of the TGN that may be involved in the transport of auxin signaling modules and/or secreted vascular formation factors.

determine which *Arabidopsis* ARF is the real substrate of VAN3. These results may cast new light on the function of ARF-GAPs. It is reported that the GAP activity of AZAP-type ARF-GAPs is controlled by phospholipids (Brown et al., 1998; Jackson et al., 2000; Kam et al., 2000). Each AZAP subfamily has a distinct phosphoinositide dependence. The GAP activity of ASAPs appears to be specifically stimulated by PA and PtdIns(4,5) P_2 . ARAPs are regulated by PtdIns(3,4,5) P_3 , and ACAPs by PtdIns(3,5) P_2 and PtdIns(4,5) P_2 (Randazzo and Hirsch, 2004). In contrast, whereas VAN3 shows an obvious affinity for PtdIns4 P and weak binding to PtdIns and PtdIns(4,5) P_2 , it shows no binding to phosphatidic acid (PA) (Fig. 5C). Although we have not yet determined the phospholipid dependency of the ARF-GAP activity of VAN3, this finding suggests differences in the phospholipid-dependent regulatory mechanism of ARF-GAP activity in animals and plants. These different lipid dependencies may also be responsible for the subcellular localization of AZAP-type ARF-GAPs. The PH or Phox homology (PX) domains can contribute to targeting a protein to a specific membrane compartment (Peter et al., 2004). Recent results suggest that the BAR domain is responsible for dimerization, membrane binding and a curvature-sensing module (Lee and Schekman, 2004; Peter et al., 2004). Interestingly, there are also reports that the BAR domain can form heterodimers *in vivo* and *in vitro* (Navarro et al., 1997; Wigge et al., 1997; Colwii et al., 1999). These results remind us that VAN3 may form not only homodimers, but also heterodimers with its homologs to cooperatively regulate the transportation of a cargo protein that regulates vascular continuity.

In animals, an ACAP member, ARF6-GAP, localized to focal adhesions and recycling endosomes (Jackson et al.,

2000). However, the VAN3 protein does not appear to function in endosomal trafficking because VAN3 co-localizes with the TGN marker SYP41 (Fig. 6G-I) and not with the endosomal marker ARA6-GFP (Fig. 6D) or the endocytic tracer FM (data not shown). This suggests that VAN3 functions in membrane trafficking at the TGN. This result was supported with transgenic plants, in which VAN3::VAN3-VENUS complemented the *van3* mutant phenotypes (data not shown). Different phospholipid dependencies may contribute to the different subcellular locations of VAN3 and ACAPs. These results imply that VAN3 is a plant-specific ACAP-type ARF-GAP that functions in transporting cargo proteins involved in distinct cellular events in plants.

Interestingly, VAN3 did not co-localize with all the cellular structures stained with the TGN marker SYP41 (Fig. 6I). This suggests the existence of functionally different TGNs. It is generally believed that the TGN has a uniform function as a sorting center where trafficking proteins are directed to the plasma membrane, endosomes and prevacuolar compartments. However, our observations suggest that the TGN may be differentiated, and therefore that the final target of the cargos may already be selected before they are delivered to the TGN (Fig. 7). This idea is consistent with the specific and restricted effects of VAN3 on vascular continuity. VAN3 homologs and/or other ARF-GAPs might be candidate regulators of alternative, or more general, TGN transporting pathways.

VAN3 may be responsible for auxin signaling

van3 pin1 double mutants have an additive phenotype, suggesting independent functions of VAN3 and PIN1 in venation pattern construction. PIN1 is responsible for polar auxin transport (Gälweiler et al., 1998), so VAN3 is not a component of the system that regulates polar auxin transport. The additional phenotypes induced by the application of the polar auxin transport inhibitors NPA and TIBA to the *van3* mutants also support the view that VAN3 functions independently of polar auxin transport-system-related vascular formation.

Expression of the *DR5::GUS* construct was not induced by the application of auxin to *van3* leaves (Fig. 3K-V). This implies that the VAN3 protein functions in auxin signaling. Because VAN3 expression was upregulated by the application of auxin, there may be positive feedback between VAN3 expression and auxin signaling. Furthermore, the enhanced *mp* phenotype (Fig. 1L) and reduced *MP* expression level in the *van3* mutants (data not shown) suggest that VAN3 may regulate auxin signaling upstream from MP.

The *gnom* mutants show a concentrated venation pattern (Fig. 1G). *GNOM* encodes an ARF-GEF that is believed to regulate the subcellular localization of PIN1 and to contribute to polar auxin transport (Geldner et al., 2003). Therefore, the concentrated venation in the *gnom* mutants may result from highly accumulated auxin in the leaf resulting from the aberrant localization of PIN1. BFA, which represses the GNOM function, induced concentrated venation, especially at the leaf margins, as occurs in the *gnom* mutants (Fig. 2I-L). The *van3* mutation partially suppressed the concentrated venation pattern in both the *gnom* and BFA-treated leaves (Fig. 1I,J, Fig. 2I-P). This observation may be explained as follows. The reduced auxin signaling caused by the *van3* mutation may suppress the overproduction of vascular tissues caused by

excess auxin accumulation in *gnom* leaves or BFA-treated leaves. How does VAN3 regulate auxin signaling? VAN3 may be responsible for the transportation of the components of intracellular auxin signaling, such as receptors or signal transduction intermediates, from the TGN. Consequently, the loss of function of VAN3 results in reduced auxin sensitivity. *DR5::GUS* expression is often used as a marker of auxin accumulation (Sabatini et al., 1999; Friml et al., 2003; Mattson et al., 2003), but more correctly shows auxin reactivity. The reduced sensitivity of auxin in the *van3* mutant is consistent with this hypothesis. However, we cannot exclude the possibility that VAN3 is involved in the trafficking of a secretory protein(s) that functions in the intercellular signaling necessary for the continuous formation of procambial cells. Xylogen is an arabinogalactan protein that is secreted from procambium cells to neighboring cells, inducing them to differentiate into vascular tissue, and its mutants show a disconnected vascular pattern (Motose et al., 2004). Therefore, xylogen might be a good candidate cargo protein of VAN3-related vesicles.

Discontinuous venation pattern in *van3* mutants

We must distinguish between the discontinuous formation of procambium and that of mature xylem cells. Although the maturation process of a xylem strand is known to occur sometimes discontinuously from the continuously formed procambium in leaves (Esau, 1965; Aloni, 2001; Pyo et al., 2004), it is still unclear whether the procambium is formed discontinuously in normal leaves. In the *van3* mutant, fragmented venation is caused by the discontinuous formation of the procambium (Koizumi et al., 2000). What is the mechanism underlying this discontinuity? Aloni et al. (Aloni et al., 2003) showed that during the development of the leaf primordium, there are orderly shifts in the sites of *DR5::GUS* expression. This progress from the elongation tip, continues downward along the expanding blade margins, and ends at the central regions of the lamina. In the lamina, as we demonstrated here, *DR5::GUS* expression occurs in small round, oval or elongated cells that are distributed separately from each other, and in some cases are attached to form a short column (Fig. 3E). These *DR5::GUS*-expressing cells appear to be procambial initials or procambial cells. In more mature leaves, *DR5::GUS* expression is observed in elongated procambial cells in veins (Aloni et al., 2003). These results suggest the following scenario for the continuous formation of procambial strands. The precursors of procambial cells are formed separately with a high level of auxin, and then differentiate into procambial cells. The procambial cells then induce neighboring parenchyma cells to differentiate into procambial cells. The resultant short columns of procambial cells become attached and form a continuous strand of procambial cells. *DR5::GUS*-expressing cells in the *van3* leaves were distributed at a lower density than those in wild-type leaves (Fig. 3A–J). In *van3* leaves, the application of auxin did not enhance *DR5::GUS* expression (Fig. 3K–V). This suggests that the *van3* mutation reduces auxin sensitivity in leaves. Auxin signaling mutants, such as *axr6* and *mp*, also show discontinuous venation patterns (Berleth and Jürgens, 1993; Hobbie et al., 2000). Because auxin induces the differentiation of procambial cells/procambial initials from parenchymal cells (Fukuda, 2004), these results imply that the

reduced sensitivity of auxin in *van3* leaves causes a decrease in the number of procambial initials that are differentiated from parenchymal cells. As a result, the increased distance between each procambial initial in the *van3* leaves may prevent them from connecting to one another, thus forming a discontinuous vascular network.

The vesicle transport system appears to play an important role in the development and environmental responses of plants. In this study, we have shown for the first time a novel AZAP-type ARF–GAP that functions in pattern formation in the plant vascular network. The location of the protein in the TGN and its role in auxin signaling provide new insight into the vesicular transport involved in vascular pattern formation. Identification of the components of the VAN3-related vesicle transport system, especially the cargo protein, is the next crucial problem to be solved.

The authors thank Dr Thomas Berleth, University of Toronto, for providing *monopteros* seeds; Dr Thomas J. Guilfoyle, University of Missouri–Columbia, for providing transgenic *Arabidopsis* seeds carrying *DR5::GUS*; and Drs Tomohiro Uemura and Masahiko Sato, Kyoto University, for plasmids containing *35S::SYP41–GFP* and *35S::VAMP727–GFP*. We also thank Dr Atsushi Miyawaki (RIKEN) for providing Venus–YFP, the *Arabidopsis* Biological Resource Center, Columbus, Ohio, for providing BAC clones, and Dr Shigeo Tanaka (Tokyo University of Agriculture) for allowing K.K. to perform experiments in his laboratory. This work was supported in part by Grants-in-Aid from the Ministry of Education, Science, Sports and Culture of Japan to H.F. (no. 14036205) and S.S. (no. 16770028), from the Mitsubishi Foundation to H.F., from the Inamori Foundation, the Yamada Science Foundation and the Nissan Science Foundation to S.S., and from the Japanese Society for the Promotion of Science to H.F. (no. 15370018).

References

- Aida, M., Vernoux, T., Furutani, M., Traas, J. and Tasaka, M. (2002). Roles of *PIN-FORMED1* and *MONOPTEROS* in pattern formation of the apical region of the *Arabidopsis* embryo. *Development* **129**, 3965–3974.
- Aloni, R. (2001). Foliar and axial aspects of vascular differentiation: hypotheses and evidence. *J. Plant Growth Regul.* **20**, 22–34.
- Aloni, R., Schwalm, K., Langhans, M. and Ullrich, C. I. (2003). Gradual shifts in sites of free-auxin production during leaf-primordium development and their role in vascular differentiation and leaf morphogenesis in *Arabidopsis*. *Planta* **216**, 841–853.
- Avsian-Kretschmer, O., Cheng, J. C., Chen, L., Moctezuma, E. and Sung, Z. R. (2002). Indole acetic acid distribution coincides with vascular differentiation pattern during *Arabidopsis* leaf ontogeny. *Plant Physiol.* **130**, 199–209.
- Bassham, D. C., Sanderfoot, A. A., Kovaleva, V., Zheng, H. and Rikhel, N. V. (2000). ATVPS45 complex formation at the trans-Golgi network. *Mol. Biol. Cell* **11**, 2251–2265.
- Benková, E., Michniewicz, M., Sauer, M., Teichmann, T., Seifertová, D., Jürgens, G. and Friml, J. (2003). Local, efflux-dependent auxin gradients as a common module for plant organ formation. *Cell* **115**, 591–602.
- Bennett, S. R. M., Alvarez, J., Bossinger, G. and Smyth, D. R. (1995). Morphogenesis in *pinoid* mutants of *Arabidopsis thaliana*. *Plant J.* **8**, 505–520.
- Berleth, T. and Jürgens, G. (1993). The role of the *monopteros* gene in organizing the basal body region of the *Arabidopsis* embryo. *Development* **118**, 575–587.
- Berleth, T., Mattsson, J. and Hardtke, C. S. (2000). Vascular continuity and auxin signals. *Trends Plant Sci.* **5**, 387–393.
- Brown, M. T., Andarade, J., Radhakrishna, H., Donaldson, J. G., Cooper, J. A. and Randazzo, P. A. (1998). ASAP1, a phospholipid-dependent Arf GTPase-activating protein that associate with and is phosphorylated by Src. *Mol. Cell. Biol.* **18**, 7038–7051.
- Busch, M., Mayer, U. and Jürgens, G. (1996). Molecular analysis of the

- Arabidopsis* pattern formation gene *GNOM*: gene structure and intragenic complementation. *Mol. Gen. Genet.* **250**, 681-691.
- Carland, F. M. and McHale, N. A.** (1996). *LOPI*: A gene involved in auxin transport and vascular patterning in *Arabidopsis*. *Development* **122**, 1811-1819.
- Carland, F. M., Berg, B. L., FitzGerald, J. N., Jinamornphongs, S., Nelson, T. and Keith, B.** (1999). Genetic regulation of vascular tissue patterning in *Arabidopsis*. *Plant Cell* **11**, 2123-2137.
- Carland, F. M., Fujioka, S., Takatsuto, S., Yoshida, S. and Nelson, T.** (2002). The identification of *CVPI* reveals a role for sterols in vascular patterning. *Plant Cell* **14**, 2045-2058.
- Colwill, K., Field, D., Moore, L., Friesen, J. and Andrews, B.** (1999). In vivo analysis of the domains of yeast Rvs167p suggests Rvs167p function is mediated through multiple protein interactions. *Genetics* **152**, 881-893.
- Cukierman, E., Huber, I., Rotman, M. and Cassel, D.** (1995). The ARF1 GTPase-activating protein: zinc finger motif and Golgi complex localization. *Science* **270**, 1999-2002.
- de Curtis, I.** (2001). Cell migration: GAPs between membrane traffic and the cytoskeleton. *EMBO Rep.* **2**, 277-281.
- Dengler, N. G.** (2001). Regulation of vascular development. *J. Plant Growth Regul.* **20**, 1-13.
- Deyholos, M. K., Corder, G., Beebe, D. and Sieburth, L. E.** (2000). The *SCARFACE* gene is required for cotyledon and leaf vein patterning. *Development* **127**, 3205-3213.
- Donaldson, J. G. and Klausner, R. D.** (1994). ARF: a key regulatory switch in membrane traffic and organelle structure. *Curr. Opin. Cell Biol.* **6**, 527-532.
- Donaldson, J. G., Radhakrishna, H. and Peters, P. J.** (1995). The ARF GTPase: defining roles in membrane traffic and organelle structure. *Cold Spring Harbor Symp. Quant. Biol.* **60**, 229-234.
- Esau, K.** (1965). *Vascular Differentiation in Plants*. 160 pp. New York, NY, USA: Holt, Rinehart and Winston.
- Franco, M., Peters, P. J., Boretto, J., Van Donselaar, E., Neri, A., D'souzaSchorey, C. and Chavrier, P.** (1999). EFA6, a *sec7* domain-containing exchange factor for Arf6 coordinates membrane recycling and actin cytoskeleton organization. *EMBO J.* **18**, 1480-1491.
- Frank, S. R., Hatfield, J. C. and Casanova, J. E.** (1998). Remodeling of the actin cytoskeleton is coordinately regulated by protein kinase C and the ADP-ribosylation factor nucleotide exchange factor ARNO. *Mol. Biol. Cell.* **9**, 3133-3146.
- Friml, J., Vieten, A., Sauer, M., Weijers, D., Schwarz, H., Hamann, T., Offringa, R. and Jürgens, G.** (2003). Efflux-dependent auxin gradients establish the apical-basal axis of *Arabidopsis*. *Nature* **426**, 147-153.
- Fukuda, H.** (2004). Signals that control plant vascular cell differentiation. *Nat. Rev. Mol. Cell Biol.* **1**, 187-198.
- Gälweiler, L., Guan, C., Müller, A., Wisman, E., Mendgen, K., Yephremov, A. and Palme, K.** (1998). Regulation of polar auxin transport by AtPIN1 in *Arabidopsis* vascular tissue. *Science* **282**, 2226-2230.
- Geldner, N., Friml, J., Stierhof, Y.-D., Jürgens, G. and Palme, K.** (2001). Auxin transport inhibitors block PIN1 cycling and vesicle trafficking. *Nature* **413**, 425-428.
- Geldner, N., Anders, N., Wolters, H., Keicher, J., Kornberger, W., Muller, P., Delbarre, A., Ueda, T., Nakano, A. and Jürgens, G.** (2003). The *Arabidopsis* *GNOM* ARF-GEF mediates endosomal recycling, auxin transport, and auxin-dependent plant growth. *Cell* **24**, 219-230.
- Geldner, N., Richter, S., Vieten, A., Marquardt, S., Torres-Ruiz, R. A., Mayer, U. and Jürgens, G.** (2004). Partial loss-of-function alleles reveal a role for *GNOM* in auxin transport-related, post-embryonic development of *Arabidopsis*. *Development* **131**, 389-400.
- Hamann, T., Mayer, U. and Jürgens, G.** (1999). The auxin-insensitive *bodenlos* mutation affects primary root formation and apical-basal patterning in the *Arabidopsis* embryo. *Development* **126**, 1387-1395.
- Hamann, T., Benková, E. and Baurle, I., Kientz, M. and Jürgens, G.** (2002). The *Arabidopsis* *BODENLOS* gene encodes an auxin response protein inhibiting *MONOPTEROS*-mediated embryo patterning. *Genes. Dev.* **16**, 1610-1615.
- Harlan, J. E., Hajduk, P. J., Yoon, H. S. and Fesik, S. W.** (1994). Pleckstrin homology domains bind to phosphatidylinositol-4, 5-bisphosphate. *Nature* **371**, 168-170.
- Hellmann, H., Hobbie, L., Chapman, A., Dharmasiri, S., Dharmasiri, N., del Pozo, C., Reinhardt, D. and Estelle, M.** (2003). *Arabidopsis* *AXR6* encodes CUL1 implicating SCF E3 ligases in auxin regulation of embryogenesis. *EMBO J.* **22**, 3314-3325.
- Hobbie, L., McGovern, M., Hurwitz, L. R., Pierro, A., Liu, N. Y., Bandyopadhyay, A. and Estelle, M.** (2000). The *axr6* mutants of *Arabidopsis thaliana* define a gene involved in auxin response and early development. *Development* **127**, 23-32.
- Huber, I., Rotman, M., Pick, E., Makler, V., Rothen, L., Cukierman, E. and Cassel, D.** (2001). Expression, purification, and properties of ADP-ribosylation factor (ARF) GTPase activating protein-1. *Methods Enzymol.* **329**, 307-316.
- Huber, I., Cukierman, E., Rotman, M. and Cassel, D.** (2002). ARF GTPase-activating protein 1. *Methods Mol. Biol.* **189**, 199-206.
- Jackson, T. R., Brown, F. D., Nie, Z., Miura, K., Foroni, L., Sun, J., Hsu, V. W., Donaldson, J. G. and Randazzo, P. A.** (2000). ACAPs are arf6 GTPase-activating proteins that function in the cell periphery. *J. Cell Biol.* **151**, 627-638.
- Jürgens, G. and Geldner, N.** (2002). Protein secretion in plants: from the *trans*-Golgi network to the outer space. *Traffic.* **3**, 605-613.
- Kam, J. L., Miura, K., Jackson, T. R., Gruschus, J., Roller, P., Stauffer, S., Clark, J., Aneja, R. and Randazzo, P. A.** (2000). Phosphoinositide-dependent activation of the ADP-ribosylation factor GTPase-activating protein ASAP1. Evidence for the pleckstrin homology domain functioning as an allosteric site. *J. Biol. Chem.* **275**, 9653-9663.
- Koizumi, K., Sugiyama, M. and Fukuda, H.** (2000). A series of novel mutants of *Arabidopsis thaliana* that are defective in the formation of continuous vascular network: calling the auxin signal flow canalization hypothesis into question. *Development* **127**, 3197-3204.
- Lee, M. C. S. and Schekman, R.** (2004). BAR domains go on a bender. *Science* **303**, 479-480.
- Makler, V., Cukierman, E., Rotman, M., Admon, A. and Cassel, D.** (1995). ADP-ribosylation factor-directed GTPase-activating protein. Purification and partial characterization. *J. Biol. Chem.* **270**, 5232-5237.
- Mattsson, J., Sung, Z. R. and Berleth, T.** (1999). Responses of plant vascular systems to auxin transport inhibition. *Development* **126**, 2979-2991.
- Mattsson, J., Kurshumova, W. and Berleth, T.** (2003). Auxin signaling in *Arabidopsis* leaf vascular development. *Plant Physiol.* **131**, 1327-1339.
- Mayer, U., Torres Ruiz, R. A., Berleth, T., Miséra, S. and Jürgens, G.** (1991). Mutations affecting body organization in the *Arabidopsis* embryo. *Nature* **353**, 402-407.
- Mayer, U., Büttner, G. and Jürgens, G.** (1993). Apical-basal pattern formation in the *Arabidopsis* embryo: studies on the role of the *gnom* gene. *Development* **117**, 149-162.
- Moss, J. and Vaughan, M.** (1995). Structure and function of ARF proteins: activators of cholera toxin and critical components of intracellular vesicular transport processes. *J. Biol. Chem.* **270**, 12327-12330.
- Moss, J. and Vaughan, M.** (1998). Molecules in the Arf orbit. *J. Biol. Chem.* **273**, 21431-21434.
- Motose, H., Sugiyama, M. and Fukuda, H.** (2004). A proteoglycan mediates inductive interaction during plant vascular development. *Nature* **429**, 873-878.
- Nagai, T., Iyata, K., Park, E. S., Kubota, M., Mikoshiba, K. and Miyawaki, A.** (2002). A variant of yellow fluorescent protein with fast and efficient maturation for cell-biological applications. *Nature Biotechnol.* **20**, 87-90.
- Navarro, P., Durrens, P. and Aigle, M.** (1997). Protein-protein interaction between the RVS161 and RVS167 gene products of *Saccharomyces cerevisiae*. *Biochem. Biophys. Acta* **1343**, 187-192.
- Nelson, T. and Dengler, N.** (1997). Leaf vascular pattern formation. *Plant Cell* **9**, 1121-1135.
- Peter, B. J., Kent, H. M., Mills, I. G., Vallis, Y., Butler, P. J., Evans, P. R. and McMahon, H. T.** (2004). BAR domains as sensors of membrane curvature: the amphiphysin BAR structure. *Science* **303**, 495.
- Przemec, G. K. H., Mattsson, J., Hardtke, C. S., Sung, Z. R. and Berleth, T.** (1996). Studies on the role of the *Arabidopsis* gene *MONOPTEROS* in vascular development and plant cell axialization. *Planta* **200**, 229-237.
- Pyo, H., Demura, T. and Fukuda, H.** (2004). Spatial and temporal tracing of vessel differentiation in young *Arabidopsis* seedlings by the expression of an immature tracheary element-specific promoter. *Plant Cell Physiol.* **45**, 1529-1536.
- Radhakrishna, H., Al-Awar, O., Khachikian, Z. and Donaldson, J. G.** (1999). Arf6 requirement for Rac ruffling suggests a role for membrane trafficking in cortical actin rearrangements. *J. Cell Sci.* **112**, 855-866.
- Randazzo, P. A. and Hirsch, D. S.** (2004). Arf GAPs: multifunctional proteins that regulate membrane traffic and actin remodeling. *Cell Signal.* **16**, 401-413.
- Randazzo, P. A., Terui, T., Sturch, S. and Kahn, R. A.** (1994). The amino terminus of ADP-ribosylation factor (ARF) 1 is essential for interaction with Gs and ARF GTPase-activating protein. *J. Biol. Chem.* **269**, 29490-29494.

- Randazzo, P. A., Terui, T., Sturch, S., Fales, H. M., Ferrige, A. G. and Kahn, R. A. (1995). The myristoylated amino terminus of ADP-ribosylation factor 1 is a phospholipid- and GTP-sensitive switch. *J. Biol. Chem.* **270**, 14809-14815.
- Randazzo, P. A., Andrade, J., Miura, K., Brown, M. T., Long, Y. Q., Stauffer, S., Roller, P. and Cooper, J. A. (2000). The Arf GTPase-activating protein ASAP1 regulates the actin cytoskeleton. *Proc. Natl. Acad. Sci. USA* **97**, 4011-4016.
- Sabatini, S., Beis, D., Wolkenfelt, H., Murfett, J., Guilfoyle, T., Malamy, J., Benfey, P., Leyser, O., Bechtold, N., Weisbeek, P. and Scheres, B. (1999). An auxin-dependent distal organizer of pattern and polarity in the *Arabidopsis* root. *Cell* **99**, 463-472.
- Sachs, T. (1991). The control of the patterned differentiation of vascular tissues. *Adv. Bot. Res. Inc. Adv. Plant Physiol.* **9**, 151-262.
- Sachs, T. (2000). Integrating cellular and organismic aspects of vascular differentiation. *Plant Cell Physiol.* **41**, 649-656.
- Sawa, S., Ohgishi, M., Goda, H., Higuchi, K., Shimada, Y., Yoshida, S. and Koshiba, T. (2002). The *HAT2* gene, a member of the HD-Zip gene family, isolated as an auxin inducible gene by DNA microarray screening, affects auxin response in *Arabidopsis*. *Plant J.* **32**, 1011-1022.
- Shevell, D. E., Leu, W. M., Gillmor, C. S., Xia, G., Feldmann, K. A. and Chua, N. H. (1994). *EMB30* is essential for normal cell division, cell expansion, and cell adhesion in *Arabidopsis* and encodes a protein that has similarity to Sec7. *Cell* **77**, 1051-1062.
- Sieburth, L. E. (1999). Auxin is required for leaf vein pattern in *Arabidopsis*. *Plant Physiol.* **121**, 1179-1190.
- Song, J., Khachikian, Z., Radhakrishna, H. and Donaldson, J. G. (1998). Localization of endogenous Arf6 to sites of cortical actin rearrangement and involvement of Arf6 in cell spreading. *J. Cell Sci.* **11**, 2257-2267.
- Steinmann, T., Geldner, N., Grebe, M., Mangold, S., Jackson, C. L., Paris, S., Gälweiler, L., Palme, K. and Jürgens, G. (1999). Coordinated polar localization of auxin efflux carrier PIN1 by GNOM ARF GEF. *Science* **286**, 316-318.
- Stevenson, J. M., Perera, I. Y. and Boss, W. F. (1998). A phosphatidylinositol 4-kinase pleckstrin homology domain that binds phosphatidylinositol 4-monophosphate. *J. Biol. Chem.* **273**, 22761-22767.
- Takeuchi, M., Ueda, T., Sato, K., Abe, H., Nagatga, T. and Nakano, A. (2000). A dominant negative mutant of Sar1 GTPase inhibits protein transport from the endoplasmic reticulum to the Golgi apparatus in tobacco and *Arabidopsis* cultured cells. *Plant J.* **23**, 517-525.
- Takeuchi, M., Ueda, T., Yahara, N. and Nakano, A. (2002). Arf1 GTPase plays roles in the protein traffic between the endoplasmic reticulum and the Golgi apparatus in tobacco and *Arabidopsis* cultured cells. *Plant J.* **31**, 499-515.
- Turner, C. E., West, K. A. and Brown, M. C. (2001). Paxillin-ARF GAP signaling and the cytoskeleton. *Curr. Opin. Cell Biol.* **13**, 593-599.
- Turner, S. and Sieburth, L. E. (2002). Vascular patterning. In *The Arabidopsis Book* (ed. C. R. Somerville and E. M. Meyerowitz). Rockville, MD: American Society of Plant Biologists.
- Ueda, T., Yamaguchi, M., Uchimiya, H. and Nakano, A. (2001). Ara6, a plant-unique novel type Rab GTPase, functions in the endocytic pathway of *Arabidopsis thaliana*. *EMBO J.* **20**, 4730-4741.
- Ueda, T., Uemura, T., Sato, M. H. and Nakano, A. (2004). Functional differentiation of endosomes in *Arabidopsis* cells. *Plant J.* **40**, 783-789.
- Uemura, T., Ueda, T., Ohniwa, R. L., Nakano, A., Takeyasu, K. and Sato, M. H. (2004). Systematic analysis of SNARE molecules in *Arabidopsis*: Dissection of the post-Golgi network in plant cells. *Cell Struct. Funct.* **29**, 49-65.
- Wigge, P., Kohler, K., Vallis, Y., Doyle, C. A., Owen, D., Hunt, S. P. and McMahon, H. T. (1997). Amphiphysin heterodimers: potential role in clathrin-mediated endocytosis. *Mol. Biol. Cell* **8**, 2003-2015.
- Willemsen, V., Friml, J., Grebe, M., van den Toorn, A., Palme, K. and Scheres, B. (2003). Cell polarity and PIN protein positioning in *Arabidopsis* require STEROL METHYLTRANSFERASE1 function. *Plant Cell* **15**, 612-625.
- Ye, Z. H. (2002). Vascular tissue differentiation and pattern formation in plants. *Annu. Rev. Plant Biol.* **53**, 183-202.